Proceedings of ASME 2018 Conference on Smart Materials, Adaptive Structures and Intelligent Systems
SMASIS 2018
September 10-12, 2018, San Antonio, TX, USA

SMASIS2018-8189

TRAVELING WAVES AS A DE-POWDERING PROCESS FOR ADDITIVELY MANUFACTURED PARTS

Charles M. Tenney[1,2]*, **Vijaya V. N. Sriram Malladi**[1], **Patrick F. Musgrave**[1], **Christopher B. Williams**[2], **Pablo A. Tarazaga**[1]

[1]Vibrations, Adaptive Structures and Testing (VAST) laboratory
Department of Mechanical Engineering
Virginia Polytechnic Institute and State University
Blacksburg, Virginia 24061

[2]Design, Research, and Education for Additive Manufacturing Systems (DREAMS) laboratory
Department of Mechanical Engineering
Virginia Polytechnic Institute and State University
Blacksburg, Virginia 24061

ABSTRACT

Steady-state traveling waves in structures have been previously investigated for a variety of purposes including propulsion of objects and agitation of a surrounding medium. In the field of additive manufacturing, powder bed fusion (PBF) is a commonly used process that uses heat to fuse regions of metallic or polymer powders within a loose bed. PBF processes require post-process removal of loose powder, which can be difficult when blind holes or complex internal geometry are present in the fabricated part. Here, a preliminary investigation of a simple part is conducted examining the use of traveling waves for post-process de-powdering of additively manufactured specimens.

The generation of steady-state traveling waves in a structure is accomplished through excitation at a frequency between two adjacent resonant frequencies of the structure, resulting in two-mode excitation. This excitation can be generated by bonded piezoceramic elements actuated by a sinusoidal voltage signal. The response of the structure is affected by the parameters of the excitation, such as the particular frequency of the voltage signal, the placement of the piezoceramic actuators, and the phase difference in the signals applied to different actuators. Careful selection of these parameters allows adjustment of the quality, wavelength, and wave speed of the resulting traveling waves.

In this work, open-top rectangular box specimens composed of sintered nylon powder and coated with fine sand are used to represent freshly fabricated parts yet-to-be cleaned of un-sintered powder. Steady-state traveling waves are excited in the specimens while variations in the frequency content and phase differences between actuation points of the excitation are used to affect the characteristics of the dynamic response. The effectiveness of several response types for the purpose of moving un-sintered nylon powder within the specimens is investigated.

INTRODUCTION

Steady-state traveling waves are characterized by continual wave propagation through a finite structure without apparent reflection at the boundary. This is in contrast to transient traveling waves, which propagate through a structure and then reflect at the boundaries. These reflected transient waves then superimpose with incoming traveling waves, forming standing waves.

Steady-state traveling waves are of particular interest, since they are implemented in nature as a means of propulsion: for example, by snakes and snails on land, and by eels in the water.

For a one-dimensional structure such as a beam, steady-state traveling waves have been generated when two point-sinusoidal-forces simultaneously excite the beam with the same frequency and magnitude, but with different phases. In this one-dimensional case, exciting at a frequency halfway between two consecutive natural frequencies with a phase difference of 90° yields a response that is the superposition of the two nearby standing wave mode shapes [1, 2]. Due to the phase difference, the result of these superimposed standing wave modes is a

*Address all correspondence to this author. Email: charten@vt.edu

steady-state traveling wave propagating in a single direction with no apparent reflection at the boundary. This method is known as two-mode excitation, and Loh [1] implements these traveling waves for propulsion.

Other studies have also used steady-state traveling waves as a means of propulsion: for example, to make a 'flying carpet' travel across a flat surface [3], or demonstrating the potential for mixing fluids in a cylinder [4], or to mimic the undulatory motion of underwater animals [5]. Additionally, it has been shown that the appearance, propagation direction, and other characteristics of a particular steady-state traveling wave depend strongly on the position of the excitation points, the frequency at which the excitation is generated, and the phase differences between the excitation signals applied to each excitation point [2, 6–12].

TEST SPECIMEN DESIGN AND INSTRUMENTATION

The test specimen used in this study, shown in Figure 1, is a shallow tray: a rectangular plate with a lip along three edges. Overall, the tray measures 152.4 × 76.2 × 7.62 mm, with a wall thickness of 1.27 mm everywhere.

FIGURE 1. Images of the the top (upper) and bottom (lower) surfaces of the tray. Two rows of piezoelectric elements (PZTs) acting as actuators can be seen: the left group near the closed end of the tray and the right group near the the open, lip-less end. Equations are representative of excitation signals to the two groups, where ϕ is the phase difference applied to the left group.

The specimen was fabricated in a 3D Systems Sinterstation machine using Farsoon FS3300 nylon powder. After fabrication, the specimen was removed from the powder bed and cleaned of excess powder. Then, the specimen was dyed vermilion so that the movement of white sand could be observed clearly. Coloration via dyeing of the specimen was chosen to avoid altering the surface finish.

To produce vibrations in the specimen, two groups of three piezoelectric elements (later referred to as 'PZTs', due to their composition) were bonded to the underside of the specimen, as shown in the bottom half of Figure 1. Each of the PZTs had dimensions of 12.5 × 22 × 0.191 mm and was cut from a single Piezo Systems PSI-5H4E wafer. The arrangement of the PZTs into two groups was intended to 'shape' the input to more effectively produce waves propagating along the long dimension of the tray. The PZTs were affixed to the bottom of the tray using cyanoacrylate 'super' glue. Copper tape was used to electrically link the PZTs in each group, and a small amount of conductive paint was used to ensure the electrical connection would stand up to sustained vibration. This method was preferred to soldering due to the risk of cracking or depoling the PZTs.

Experimental setup

The experimentation proceeded in two sections: laser vibrometer testing to measure the dynamic response of the tray under a broad range of excitation signals, then sand-removal testing where several promising excitation signals were tested for their ability to move sand across the tray surface. During both sections of testing, the instrumented tray was suspended on two lengths of monofilament line. This boundary condition simulates a free boundary condition, and was chosen to be relatively insensitive to the precise position of the tray during testing. The whole assembly was then placed on a vibration-isolating granite block.

In the first test section, the assembly was observed by a Polytec PSV-400 scanning laser vibrometer, as shown in Figure 2. The laser vibrometer measures the velocity of a surface parallel to the direction of observation, and therefore measures the velocity normal to the plate surface in the shown configuration. Excitation signals were produced by a Polytec signal generator during this section and passed through an amplifier before exciting the bonded PZTs.

During the following sand-removal section, the excitation was generated by an NI-9263 output card and then amplified. Images of the tray surface were extracted from video captured by a camera mounted above the tray. Otherwise, the setup was the same as the previous section.

EXPERIMENTS AND RESULTS

As discussed above, the testing proceeded in two main sections: measurement of the tray's dynamic response using a laser vibrometer, and video recording of the movement of white sand

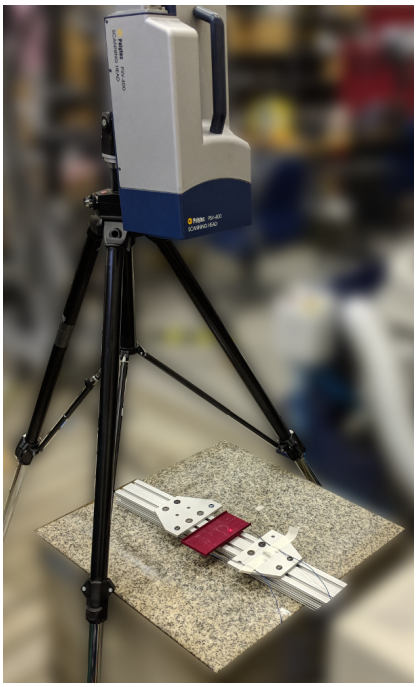

FIGURE 2. **Images of the test setup (left) and the top (upper right) and bottom (lower right) surfaces of the tray. On the bottom surface of the tray, the two rows of PZTs acting as actuators can be seen.**

spread over the tray surface. The ultimate goals of the laser vibrometer testing were to identify excitation frequencies that 1) produced steady-state traveling waves, 2) produced a large amount of surface velocity, and 3) propagated from the closed left side towards the open right side of the tray. The sand-removal testing would then experimentally demonstrate the effectiveness of those identified excitation frequencies at moving sand across the tray surface.

Frequency selection criteria

In this work, the goal is to produce propulsion across the tray surface. At the outset, this was thought to be largely dependent on three variables: surface velocity, surface curvature, and the relative magnitudes of the traveling and standing wave responses. Conceptually, the surface velocity would determine how much the sand moved, the curvature would determine the vector along which the sand was moved, and the prominence of the traveling wave component would influence the overall bias in the direction of movement.

For the purposes of de-powdering, it was thought that maximizing the traveling wave behavior of the tray was most important. In practice, this meant that the variance in the root-mean-square surface velocity was to be minimized. This is the opposite of a standing wave response where the root-mean-square surface velocity is highly variable: essentially zero along nodal lines and large at the anti-nodes, allowing the particulate to settle along the nodal lines. Of secondary concern were the surface velocity and the surface curvature, which were thought to only affect the speed at which the de-powdering occurred.

During the laser vibrometer testing, there were three main concerns that limited the range of frequencies investigated. First, a lower bound of several hundred hertz is a practical limitation of the PZTs used for actuation, due to the very limited amount of displacement available. Second, the laser vibrometer takes data at one point at a time, and must sample over a grid of points to reconstruct the vibration of the entire surface. For a deflection shape to be well resolved, the density of scan points must be sufficiently smaller than the wavelength of the vibration. Third, the signal generator used during sand-removal testing only reproduced waveforms at a 100 kHz sampling frequency, which meant that fine control of the phase difference between signals and the quality of the waveform itself were significantly reduced above 10 kHz.

Laser vibrometer measurement and investigation of traveling waves

The dynamic response of the tray was collected over an evenly spaced rectangular grid of 1817 points with nodes approximately 5 mm apart. At each point, the tray was excited by a chirp signal with a 2V amplitude (4V peak-to-trough) containing frequencies from 400-20,000 Hz. The response was recorded by the laser vibrometer at each point. Use of the Polytec signal generator allowed the automatic computation of dynamic response data for a wide range of frequencies, but could not vary the phase between output channels in the software. Therefore, this process was performed only twice: once with the two PZT groups excited in phase, and once with the phase of the signal to the left-end PZT inverted by manually reversing the positive and negative leads. In Figure 1, this corresponds to ϕ equal to 0 for the in-phase case and equal to π for the out-of-phase case. Making changes to this test setup that allow automation of the wide-spectrum testing of other phase differences is certainly worth exploring further, particularly for AM specimens where computer modeling is made difficult by complex geometry and non-isotropic material properties.

The collected data were processed to yield a complex velocity at each measurement point over a range of frequencies. In Figure 3, the magnitude of the complex velocities are averaged over the plate surface at each frequency for the in-phase case. In the figure, four circles indicate the frequencies of interest discussed later in this paper. Two frequencies (6116 Hz and 7714 Hz) are located at peaks in the plot, indicating that they produce standing waves for this combination of actuator position, frequency, and phase difference. The other two frequencies (7385 Hz and 9153 Hz) are located between peaks, as any steady-state traveling wave frequency must be.

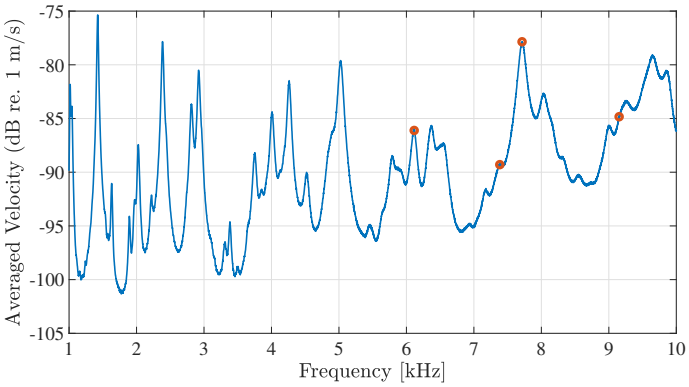

FIGURE 3. **Magnitude of complex velocity averaged over all measurement points. Circles indicate frequencies for which sand-removal is shown in the following sections.**

However, due to the fact that *any* frequency not on a peak has some combination of standing and traveling wave components, a method is needed to evaluate the quality of the traveling wave response. The method used here has to do with the nodal lines present in the standing wave response. When the response is dominated by the standing wave component, the range of velocity magnitudes is greatest due to the lack of response at the nodes, as can be seen clearly in the 7714 Hz response in Figure 4. As the traveling component becomes dominant, the range of velocity magnitudes shrinks because the propagation of the wave spreads the vibration evenly across the surface, seen most clearly in the 9153 Hz response in Figure 4.

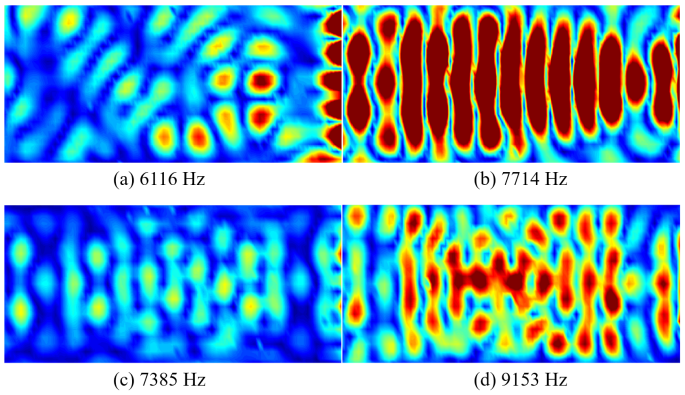

FIGURE 4. **Magnitude of complex velocity over tray surface at four frequencies. The top row (a-b) shows two frequencies at which the response is primarily a standing wave. The lower row (c-d) shows two frequencies at which significant steady-state traveling wave behavior was obtained.**

To further narrow the candidate frequencies, it was desirable to select traveling waves that primarily propagated along the length of the tray, as opposed to circulating within a confined region in the tray. To visualize the propagation, an approximation of the time-domain response at a single frequency was computed. With knowledge of the complex velocity at each point and at each frequency, the time-domain response of the tray can be simulated by computationally incrementing the phase angle of the response at every point. The result of this process is shown in Figure 5 for one standing wave frequency and one traveling wave frequency to illustrate the difference.

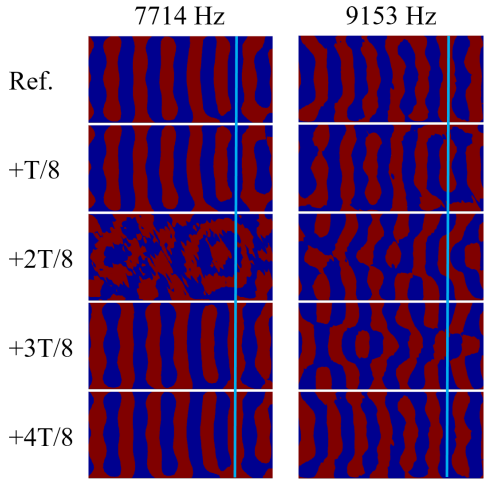

FIGURE 5. **Surface velocity plots for a standing (left) and traveling (right) wave at several points over their period, T. Values are thresholded to show in/out of page direction only. Blue lines are superimposed to help compare position across images. For the 7714 Hz standing wave, the pattern is stationary before 1/4 period, then rapidly changes, then is stationary with the velocities reversed. For the 9153 Hz traveling wave, the pattern along the centerline of the tray gradually shifts from right to left.**

Some frequencies with traveling wave behavior produced circulating propagation that did not produce a net bias to the movement of sand across the surface. After eliminating frequencies with these primarily circulating steady-state traveling waves, several frequencies of interest were selected among those frequencies producing propagation along the length of the plate. For these remaining frequencies, the response of the tray was recorded with the laser vibrometer as the phase difference between the PZT groups was varied. The purpose of this was to further enhance the traveling component of the response. As before, the even distribution of velocity magnitude across the tray surface was the quality we sought to increase.

Due to the previously mentioned limitations of the setup

used, the phase variation was accomplished by generating the excitation with the NI output card, which was sufficient for testing at individual frequencies. After testing in 5° increments, the final frequencies and phases discussed in the following section are listed in Table 1. The phase listed is the same as the ϕ shown in Figure 1.

TABLE 1. Excitation Parameters

Frequency	Initial Phase	Final Adjusted Phase
7385 Hz	0°	-20°
9153 Hz	180°	185°

Testing motive power

In this section, we will examine the frequencies identified previously: the two frequency/phase combinations listed in Table 1 as well as two standing wave frequencies for the sake of comparison. For these frequency/phase combinations, initial experimentation was performed to determine effectiveness at removing sand from the tray surface. During the test, the tray was set up in the same way as the laser vibrometer testing. The excitation in all cases was applied to the PZTs at a 20V amplitude (40V peak-to-trough) and for a 40 second duration. It is assumed here that the behavior of the tray is linear at the tested amplitudes: deflections on the order of microns during the 2V chirp.

This test provides a practical comparison of performance at different frequencies. However, quantitative comparisons should not be drawn from it. The reason for this is the non-perfect flatness of the tray. As can be seen in Figure 1, it is bowed in the center such that the ends are slightly lower than the center. Fabrication of a new, flatter tray is worth further investigation and testing.

The results show a range of effectiveness. At 6116 Hz, the standing wave pattern is not very orderly, and the sand is not effectively moved off of the tray. It does fall towards the nodal lines, but does not move from there. At 7714 Hz the standing wave pattern serves to first push the sand towards nodal lines. Then, due to the orientation of the nodal lines and high vibration near the center of the plate generally, the sand flows along the nodal lines towards the edges of the tray.

The traveling-wave response at 7385 Hz performs similarly to the standing wave at 7714 Hz. However, the 7385 Hz response accomplishes this with lower amplitude and while clearing a more rectangular-shaped region. This may indicate that the distributed and directional vibration of a steady-state traveling wave can more efficiently move the loose sand. The 9153 Hz excitation improves upon the 7385 Hz performance, being both more effective at clearing the edges of the tray and seeming most effective overall at moving the sand away from the center of the tray.

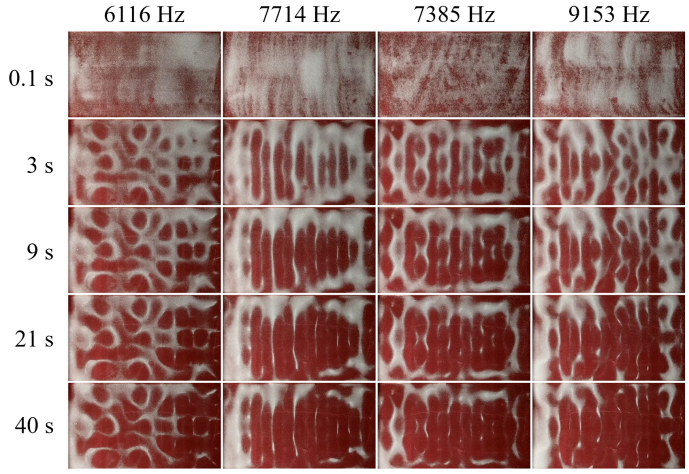

FIGURE 6. **Images of sand removal effectiveness at selected frequencies. Each column shows the progress of sand removal as excitation time increases. In the left two columns, the two standing wave frequencies, and in the right two columns, the two traveling wave frequencies are shown.**

CONCLUSION

In this paper, the use of steady-state traveling waves is explored as a conceptual means of removing excess powder from 3D printed parts. Towards this end, a shallow tray-shaped test specimen was fabricated through a powder-bed fusion process. The dynamic response of the tray was first collected under excitation by bonded piezoelectric elements through use of a scanning laser vibrometer. Then, desirable responses were selected from the vibrometer data and reproduced to gauge their effectiveness in removing fine sand from the tray surface. It was found that, depending on the structure of the wave pattern, both standing waves and steady-state traveling waves showed some capability of moving sand across the surface.

However, the result is not without qualifications. Ideally, further investigation would reveal some frequency/phase combination that produces both orderly patterns of deflection and uniform traveling wave propagation across the entire tray surface. Additionally, the effectiveness of the frequencies discussed above is difficult to gauge, since the non-flatness of the tray surface influences the movement of the sand. Finally, the placement of the actuators – the third major contributor to the shape, direction, and quality of steady-state traveling waves [10, 11] – was not changed over the course of this test. Going forward, the clearest next steps are to investigate 1) ways to excite and evaluate a wider range of frequencies and phase differences ef-

ficiently, 2) the effect of positioning on traveling wave quality, and 3) the combination of multiple frequencies of excitation to produce more uniform propagation across the surface.

Despite these qualifications, it is clear that some response shapes are more effective at moving sand than others. Through further development, it is possible that steady-state traveling waves could be used to complement current de-powdering techniques. In the long term, problems that are currently very difficult, such as clearing curved internal channels, could potentially be better addressed by steady-state traveling wave de-powdering.

ACKNOWLEDGMENT

This material is based upon work supported by the National Science Foundation under Grant Number CMMI-1635356. Any opinions, findings, and conclusions or recommendations expressed in this material are those of the author(s) and do not necessarily reflect the views of the National Science Foundation. Dr. Tarazaga would like to acknowledge the support provided by the John R. Jones III Faculty Fellowship.

REFERENCES

[1] B. G. Loh and P. I. Ro, "An object transport system using flexural ultrasonic progressive waves generated by two-mode excitation," *IEEE Transactions on Ultrasonics, Ferroelectrics, and Frequency Control*, vol. 47, no. 4, pp. 994–999, 2000.

[2] V. V. N. S. Malladi, D. Avirovik, S. Priya, and P. A. Tarazaga, "Travelling Wave Phenomenon Through Piezoelectric Actuation Of A Free- Free Beam," in *Smart Materials, Adaptive Structures and Intelligent Systems*, 2014.

[3] N. T. Jafferis, H. A. Stone, and J. C. Sturm, "Traveling wave-induced aerodynamic propulsive forces using piezoelectrically deformed substrates," *Applied Physics Letters*, vol. 99, no. 11, 2011.

[4] A. Phoenix, V. V. N. S. Malladi, and P. A. Tarazaga, "Traveling Wave Phenomenon Through Piezoelectric Actuation Of A Free-Free Cylindrical Tube," in *Smart Materials, Adaptive Structures and Intelligent Systems*, 2015.

[5] V. V. N. S. Malladi, M. Albakri, P. Musgrave, and P. A. Tarazaga, "Investigation of propulsive characteristics due to traveling waves in continuous finite media," in *Proc. SPIE 10162*, no. April 2017, 2017.

[6] V. V. Malladi, D. Avirovik, S. Priya, and P. Tarazaga, "Characterization and representation of mechanical waves generated in piezo-electric augmented beams," *Smart Materials and Structures*, vol. 24, no. 10, 2015.

[7] V. V. N. S. Malladi, M. Albakri, S. Gugercin, and P. A. Tarazaga, "Reduced Plate Model Used For 2d Traveling Wave Propagation," in *Smart Materials, Adaptive Structures and Intelligent Systems*, 2018.

[8] D. Avirovik, V. V. Malladi, S. Priya, and P. A. Tarazaga, "Theoretical and experimental correlation of mechanical wave formation on beams," *Journal of Intelligent Material Systems and Structures*, vol. 27, no. 14, pp. 1939–1948, 2016.

[9] V. V. S. Malladi, M. Albakri, and P. A. Tarazaga, "An experimental and theoretical study of two-dimensional traveling waves in plates," *Journal of Intelligent Material Systems and Structures*, vol. 28, no. 13, pp. 1803–1815, 2017.

[10] V. V. S. Malladi, M. I. Albakri, S. Gugercin, and P. A. Tarazaga, "Application of projection-based model reduction to finite-element plate models for two-dimensional traveling waves," *Journal of Intelligent Material Systems and Structures*, vol. 28, no. 14, pp. 1886–1904, 2017.

[11] P. Musgrave, V. Malladi, and P. Tarazaga, "Investigation into the superposition of multiple mode shape composed traveling waves," in *Proc. SPIE*, vol. 10164, 2017.

[12] P. F. Musgrave, M. I. Albakri, and P. A. Tarazaga, "Traveling wave generation on a clamped , thin plate with flush-mounted piezoelectric actuators," in *SEM IMAC XXXVI*, 2018.